Electronic Supporting Information

Locating the Binding Domains in a Highly Selective Mixed Matrix Membrane *via* Synchrotron IR Microspectroscopy

Nicholas M. Jacques,[1] Peter R. E. Rought,[1] Detlev Fritsch,[2] Mathew Savage,[1] Harry G. W. Godfrey,[1] Lei Li,[1] Tamoghna Mitra,[3] Mark Frogley,[4] Gianfelice Cinque,[4] Sihai Yang[1]* and Martin Schröder[1]*

1. School of Chemistry, University of Manchester, Oxford Road, Manchester, M13 9PL, UK. Sihai.Yang@manchester.ac.uk; M.Schroder@manchester.ac.uk

2. Fraunhofer IAP, FB3, Geiselbergstrasse 69, Potsdam-Golm, 14476, Germany.

3. Department of Chemistry, University of Liverpool, Liverpool, L69 7ZD, UK.

4. Diamond Light Source, Harwell Science and Innovation Campus, Didcot, Oxfordshire, OX11 0DE, UK.

ESI Index

S1. Membrane Fabrication

A solution casting method was employed for the fabrication of the MFM-300(Al)/6FDA-Durene-DABA (8.5/1.5) MMM. MFM-300(Al) powder (200 mg) was dispersed in $CHCl_3$ (5 mL) with sonication and stirring, an this was followed by addition of 6FDA-Durene-DABA (8.5/1.5) (600mg) in $CHCl_3$ (10 mL). Dimethoxysilylpropyl modified poly(ethyleneimine) (20 µL) was added to the casting solution as a surface modifier and the mixture was stirred for 24 h. The mixture was evaporated to 5-7 mL and cast on a PTFE substrate and the solvent evaporated at room temperature. The membrane was subsequently treated with MeOH over a period of 12 h and the resultant free-standing MMM was dried in a vacuum oven at 120 °C for 12 h to remove trace solvents from membran prior to the permeation measurements.

S2. Membrane analysis

S2.1 PXRD analysis of MFM-300(Al)/6FDA-TMP-DABA (8.5/1.5)

PXRD analysis was conducted on the membrane on a Philips X'Pert XRD using Cu-Kα radiation to ensure retention of structure and crystallinity of the MOF once incorporated into the MMM (Figure S2).

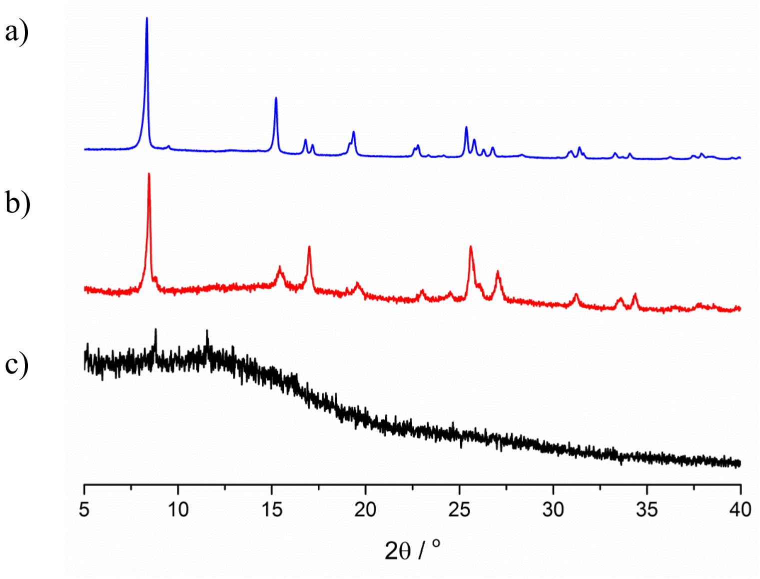

Figure S1: PXRD patterns showing the retention of crystallinity of the MOF within the membrane post-casting. a) PXRD of MFM-300(Al), b) PXRD of the 25 wt% MFM-300 (Al)/6FDA-Durnene-DABA, c) PXRD of the bare 6FDA-Durene-DABA polymer.

S2.2 SEM analysis of MFM-300(Al)/6FDA-TMP-DABA (8.5/1.5)

SEM analysis of the membrane morphology and MOF distribution was conducted at the Fraunhofer IAP.

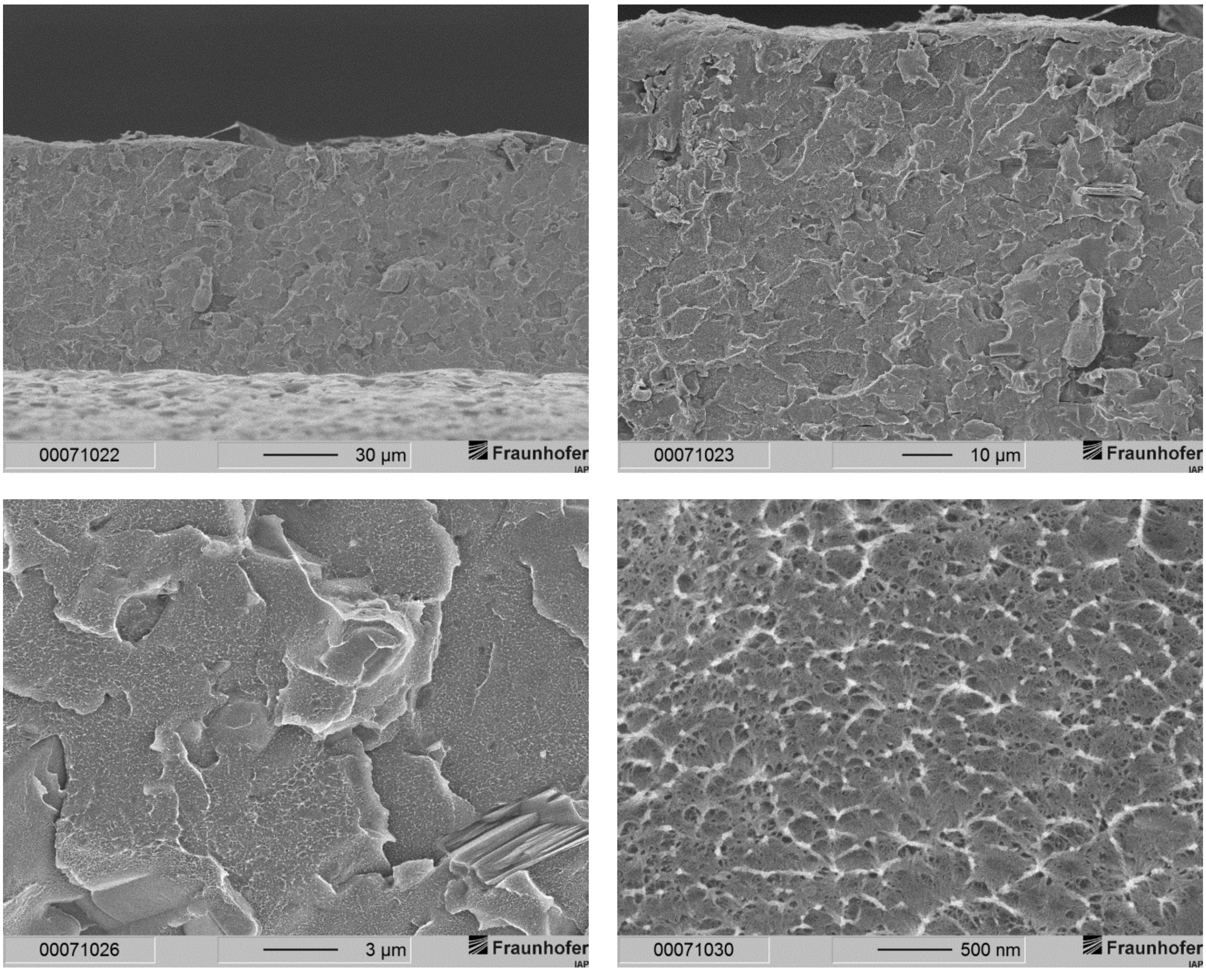

Figure S2. SEM images of the membrane cross-section showing the distribution of MOF particles in the polymer matrix and the excellent affinity between the polymer matrix and MOF particles.

S2.3 EDX analysis of MFM-300(Al)/6FDA-TMP-DABA (8.5/1.5)

The filler distribution in the membrane morphology was studied by EDX spectroscopy using a Zeiss Scanning Electron Microscope with an Energy Dispersive X-ray (EDX) detector and tungsten electron source. The membrane cross section was prepared *via* freeze fracturing using liquid N_2. The sample was then coated with carbon *via* sputtering.

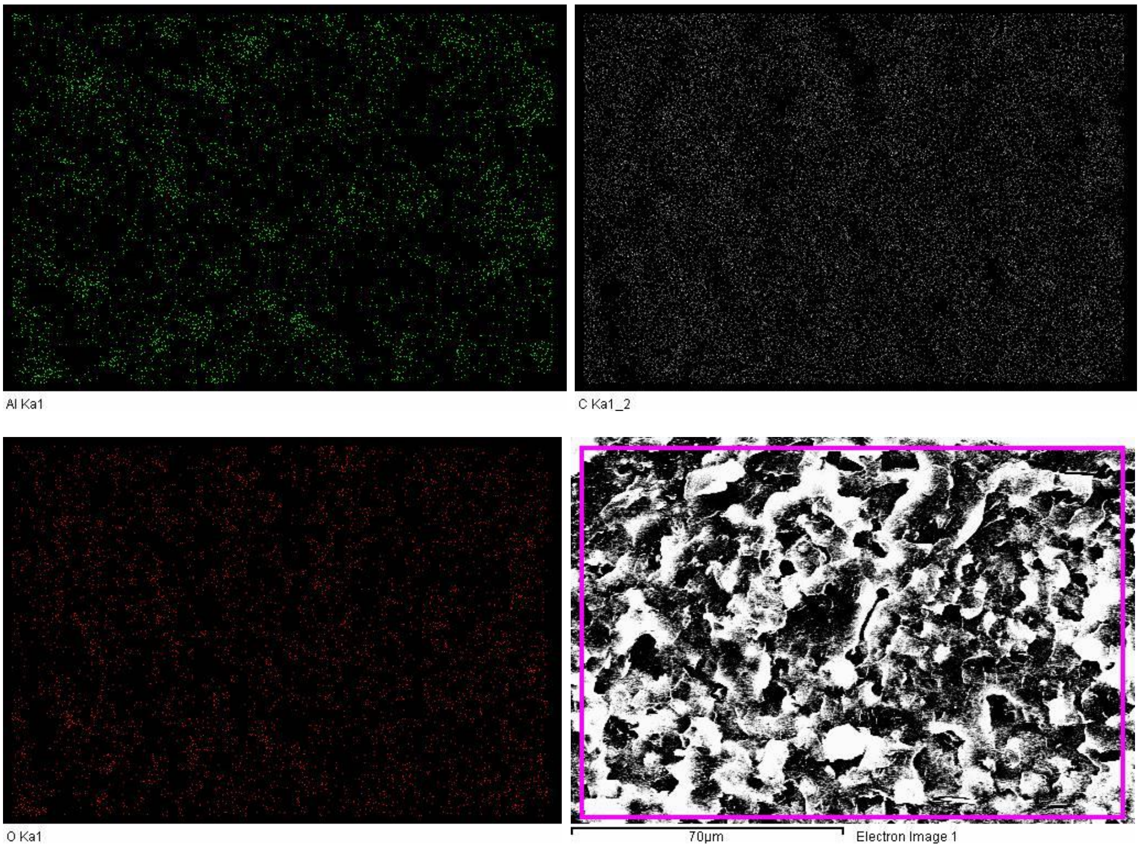

Figure S3. EDX images of the membrane cross-section showing the distribution of MOF particles in the polymer matrix.

S3. Permeation measurements

S3.1 Experimental details

Permeation measurements were conducting using the time lag method on a custom permeation rig at Fraunhofer IAP (Figure S4). Pressure gradients on the permeate side of the cell were measured using a five decimal place pressure transducer. A disk of membrane 4.5 cm diameter was placed in the cell and the permeate side evacuated using a turbo molecular pump prior to each measurement. All gas measurements were repeated three times to ensure precision in the data and N_2 was run before and after all gases had been run to ensure integrity of the membrane. The membrane thickness was measured using a micrometre and measurements from numerous sites on the membrane where taken and averaged to determine the thickness for permeation data analysis. Average thickness of the membrane was determined to be 161.7 µm.

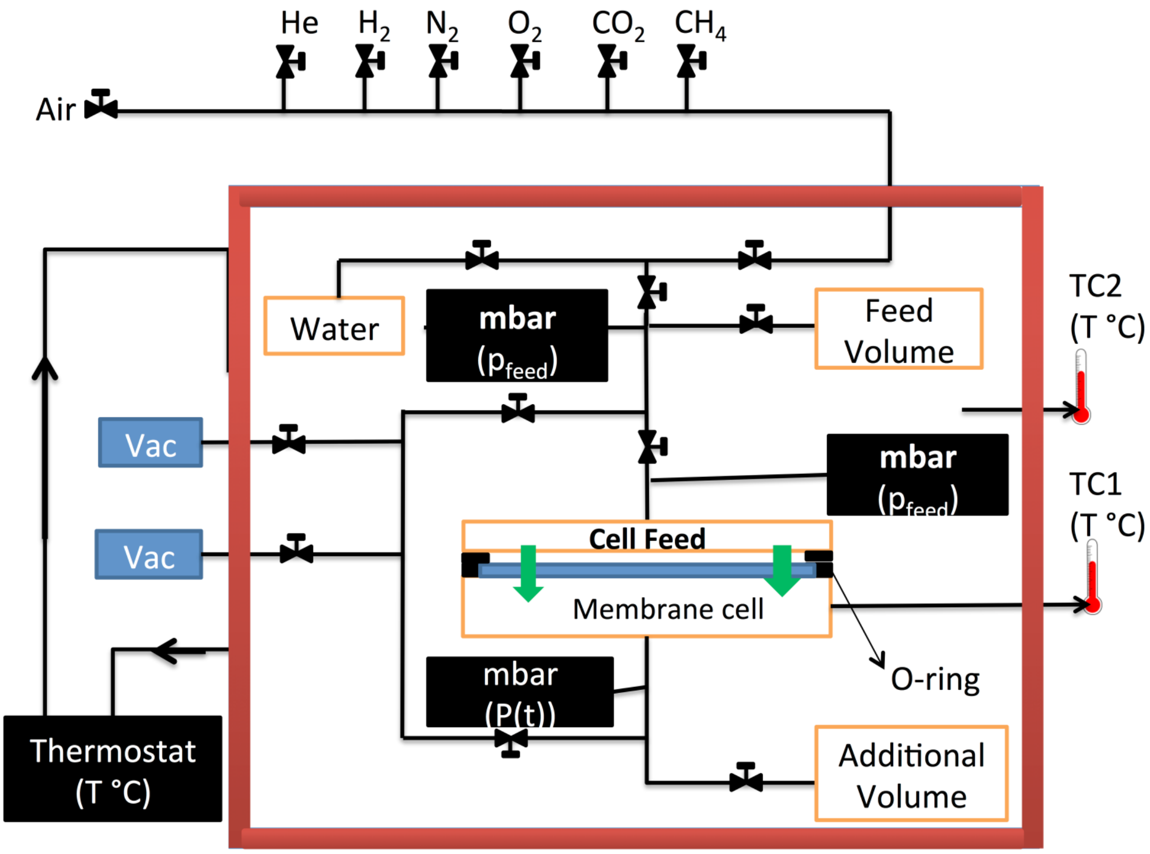

Figure S4. Schematic of the gas permeation rig used in this study.

S3.2 Results

Table S1: Results of the single gas permeation measurements for H_2, He, N_2, CO_2, O_2 and CH_4 at 30 °C.

Gas	**Permeability coefficient of bare polymer (Barrer)**	**Solubility coefficient of bare polymer (cm^3(STP) cm^2 atm^{-1})**	**Diffusion coefficient of bare polymer (x10^8 cm^2 s^{-1})**	**Permeability coefficient of MMM (Barrer)**	**Solubility coefficient of MMM (cm^3(STP) cm^2 atm^{-1})**	**Diffusion coefficient of MMM (x10^8 cm^2 s^{-1})**
H_2	282	0.19	1497	663	0.33	1992
He	221	0.07	3088	438	0.09	4782
N_2	26.6	0.80	33.9	39.1	1.02	38.3
CO_2	602	26.1	23.1	911	31.5	28.9
O_2	88.5	1.10	83.7	145	1.31	111
CH_4	34.3	1.08	32.2	27.7	2.33	11.9

S3.3 Comparisons to other 6FDA-based membranes

Table S2: Comparison of the permeability and selectivity of the MMM reported in this work to other membranes studied for CO_2/CH_4 separation in the literature.

Polymer	**Filler**	**Loading (wt%)**	P_{CO2} **/ Barrer**	**α (CO_2/CH_4)**	**Operational Conditions**	**Reference**
6FDA-Durene-DABA (8.5/1.5)	MFM-300(Al)	25	911	32	303 K, 0.75 bar	This work
6FDA-DAM	ZIF-90	15	720	37	298 K, 2 bar	1
6FDA-DAM	ZIF-11	20	257	31	303 K, 4 bar	2
6FDA-Durene-DABA (9/1)	ZIF-8	40	779	20	308, 10 bar	3
6FDA-durene	ZIF-8	5	693	16.5	303 K, 3.5 bar	4
6FDA-durene	Zeolite T	1	843	19	303 K, 3.5 bar	5
PIM-1	UiO-66-NH_2	9.1	4337	28	298 K, 1 bar	6
PIM-1	ZIF-8	36	6820	13	295 K, 1 bar	7
Matrimid 5218	ACOF-1	16	15	32	308 K, 4 bar	8
Matrimid 5218	MOF-5	30	20	29	308 K, 2 bar	9

S4. Synchrotron IR Microspectroscopy

S4.1 Experimental details

Infrared micro-spectroscopy experiments were carried out using the B22: Multimode InfraRed Imaging and Microspectroscopy (MIRIAM) beam line at the Diamond Light Source, Harwell Science Campus (UK). The instrument is comprised of a Bruker Hyperion 3000 microscope in transmission mode, with a 15x objective and liquid nitrogen cooled MCT detector, coupled to a Bruker Vertex 80 V Fourier Transform IR interferometer using radiation generated from a bending magnet source. Spectra were collected (512 scans) in the range 500-4000 cm^{-1} with 4 cm^{-1} resolution and an infrared spot size at the sample of approximately 20 × 20 μm. Portions (2 mm x 2mm) of MFM-300(Al)/6FDA-Durene-DABA (8.5/1.5) and bare 6FDA-TMP-DABA (8.5/1.5) were placed onto a

ZnSe disk and placed within a Linkam FTIR 600 gas-tight sample cell equipped with ZnSe windows, a heating stage and gas inlet and outlets. The N_2 and CO_2 were pre-dried using individual zeolite filters. The analysis gases were dosed volumetrically to the sample cell using mass flow controllers, the total flow rate being maintained at 100 cm^3min^{-1} for all experiments. The gases were directly vented to an exhaust system and the total pressure in the cell was therefore 1 bar for all experiments. The sample was desolvated under a flow of dry N_2 at 100 cm^3min^{-1} and 393 K for 2 h. The sample was then cooled to 303 K under a continuous flow of N_2. Dry N_2 and CO_2 were dosed as a function of partial pressure, maintaining a total flow of 100 cm^3min^{-1}. It is worth noting that a number of factors can affect the signal/noise ratio due to the sensitivity of synchrotron powered FTIR including the thickness of the sample and scattering effects due to the sample and the proximity of the beam to the edge of the cell aperture. Therefore, it was important to take these factors into account when selecting an appropriate area for investigation.

S4.2 IR peak fitting

The IR spectra for the bare polymer were fitted to 4 bands using a Lorentzian peak fit in OrginPro 8 data analysis software. These represent the spectrum background, the combination bands of CO_2 at 3591 cm^{-1} and 3697 cm^{-1} and the overtone of the imide C=O at 3499 cm^{-1}. This fitting allows the analysis of the change in peak area with increasing CO_2 loading.

The IR spectra of the MMM were similarly fitted using the same Lorentzian peak fit with additional peaks for the imine stretch (from the surface modifier) at 3557 cm^{-1}, the bridging hydroxyl stretch at 3693 cm^{-1} and the –OH---CO_2 stretch at 3696 cm^{-1}.

S4.3 IR Data

S4.3.1 IR spectra of surface modifier

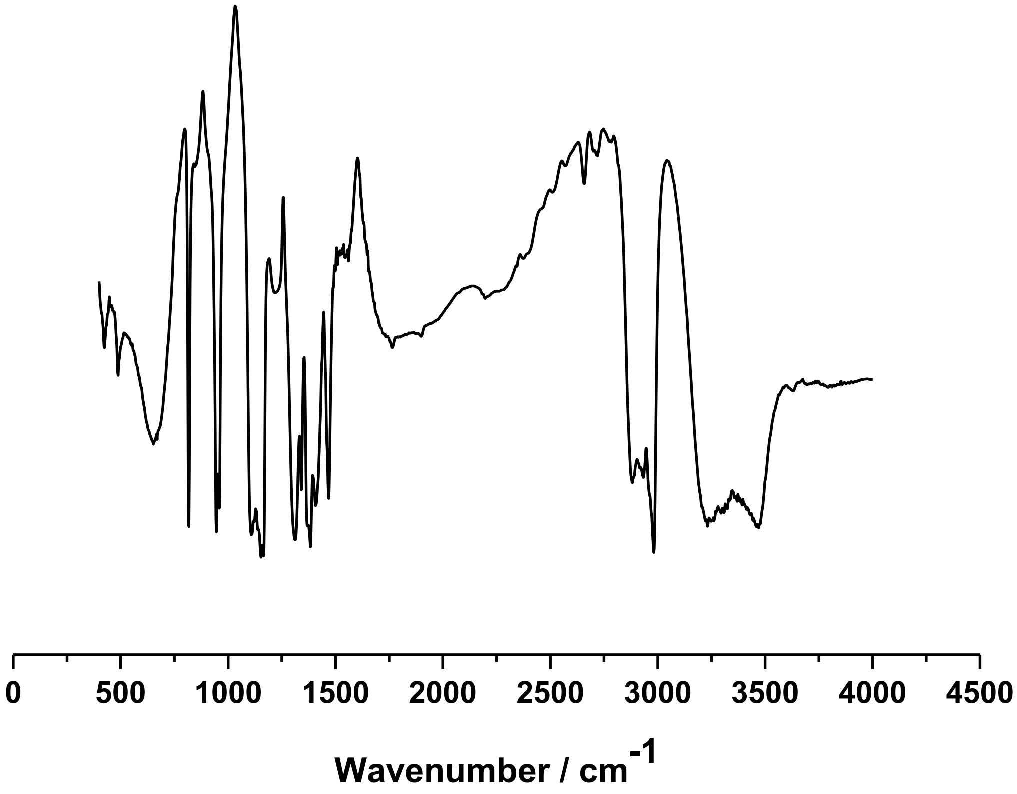

Figure S5: IR spectrum of the bare surface modifier collected from 500 to 4000 cm^{-1}.

S4.3.2 Bare 6FDA-TMP-DABA (8.5/1.5)

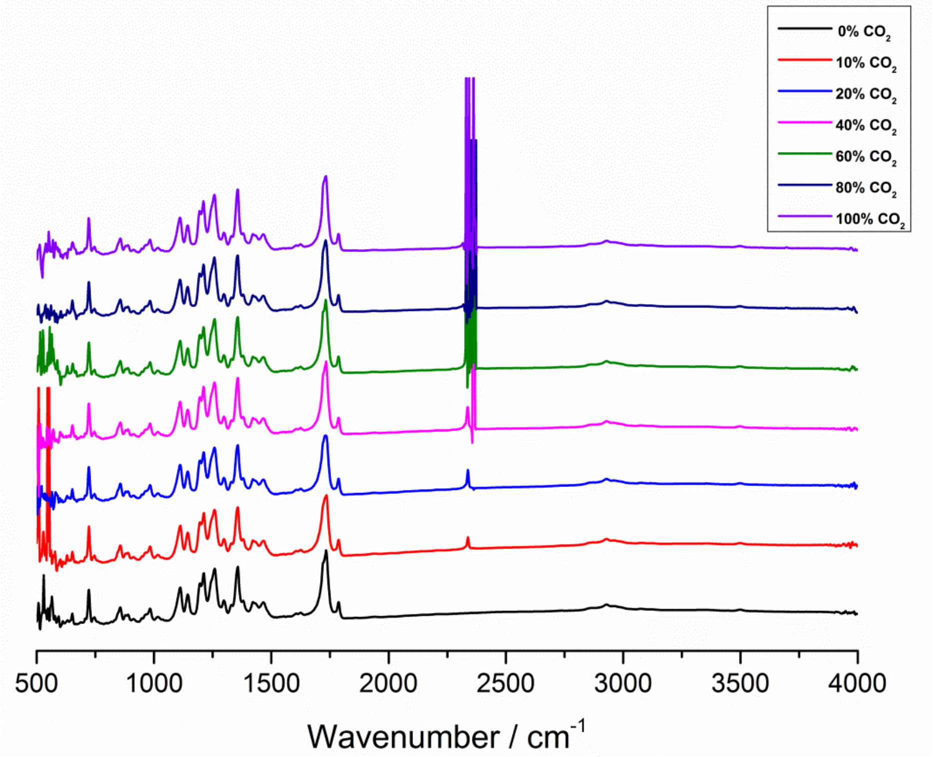

Figure S6: IR data collected from 500 to 4000 cm^{-1} for the bare polymer membrane with increasing loading of CO_2.

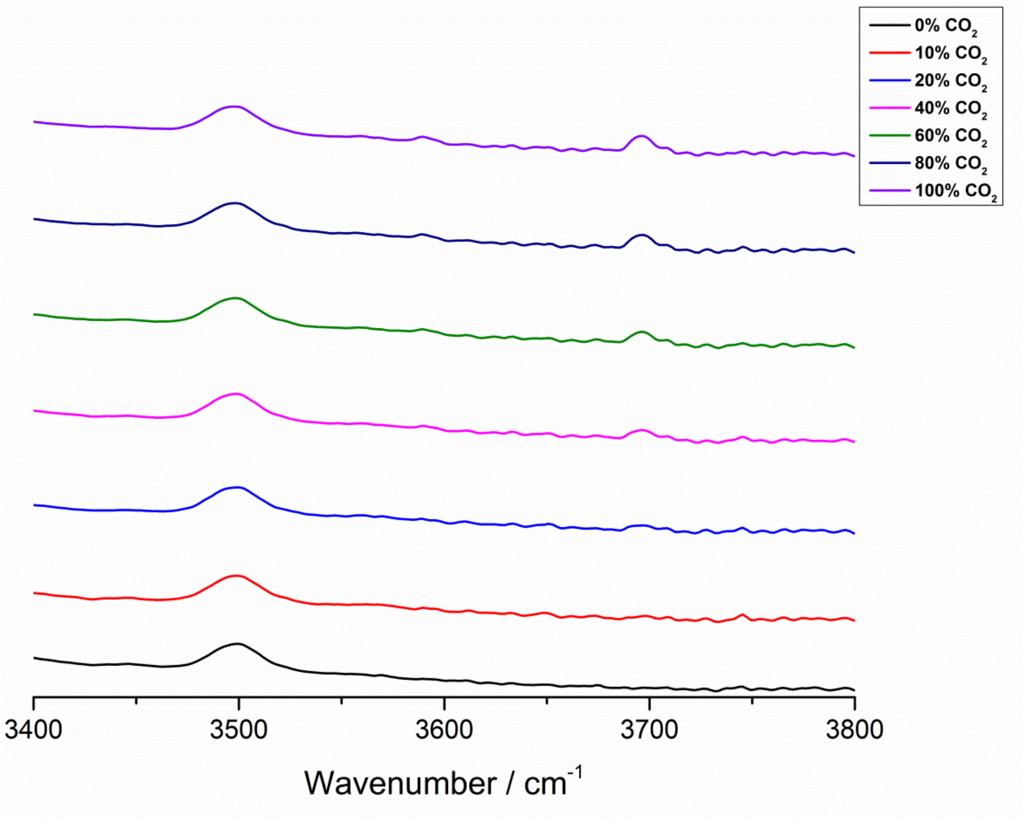

Figure S7: IR data collected for the bare polymer membrane with increasing loading of CO_2, focussing on the region of the imide overtone and CO_2 combination bands.

S4.3.3 MFM-300(Al)/ 6FDA-TMP-DABA (8.5/1.5)

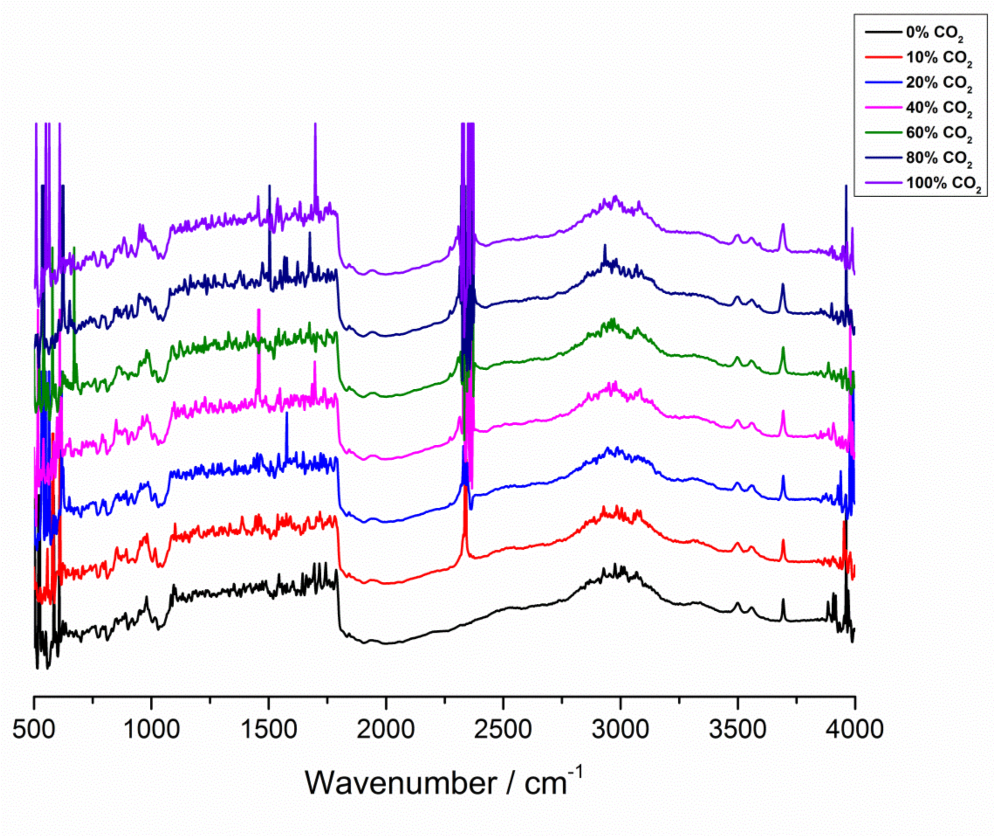

Figure S8: IR data collected from 500 to 4000 cm^{-1} for the MMM with increasing loading of CO$_2$.

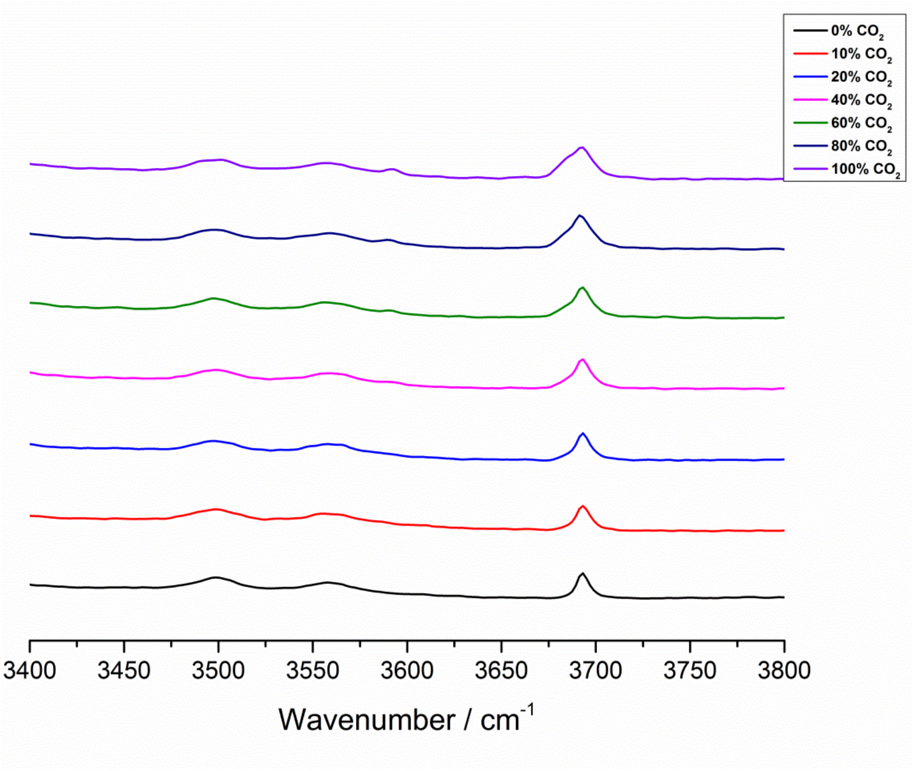

Figure S9: IR data collected for the MMM with increasing loading of CO_2 focussing on the region of bridging –OH in the pore of the MOF. The imide overtone band is attributed to the polymer and the CO_2 combination bands.

S4.3.4 $^{13}CO_2$ IR data

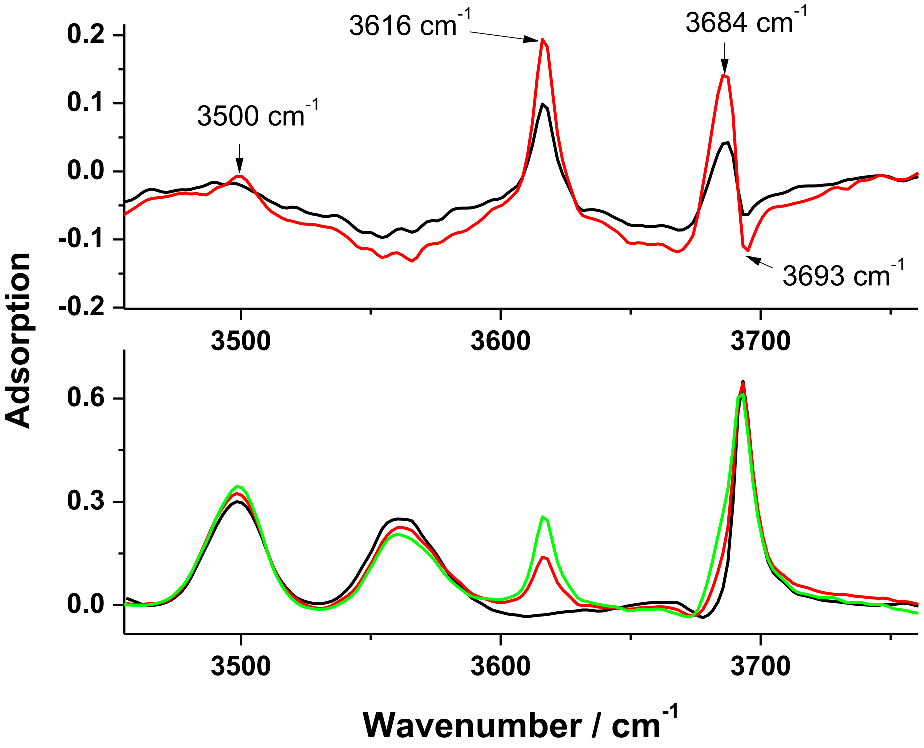

Figure S10: $^{13}CO_2$ micro-FTIR spectra. (top) Difference spectra showing the growth of new peaks at 3500 cm^{-1} and 3616 cm^{-1} of the CO_2 combination bands and a new peak at 3684 cm^{-1} together with depletion of the hydroxyl peak at 3693 cm^{-1} consistent with CO_2 binding (black = 25%, red = 50%). (bottom) Baseline subtracted spectra with increasing $^{13}CO_2$ loading (black = 0%, red = 25%, green = 50% CO_2).

5. References

1. T. H. Bae, J. S. Lee, W. Qiu, W. J. Koros, C. W. Jones, S. Nair, *Angew. Chem. Int. Ed.*, 2010, **49**, 9863–9866.

2. M. S. Boroglu, A. B. Yumru, *Sep. Purif. Technol.,* 2017, **173**, 269-279.

3. M. Askari, T.-S. Chung, *J. Membr. Sci.,* 2013, **444**, 173-183.

4. N. Jusoh, Y. F. Yeong, W. L. Cheong, K. K. Lau, A. M. Shariff, *J. Ind. Eng. Chem.*, 2016, **44**, 164-173.

5. N. Jusoh, Y. F. Yeong, K. K. Lau, A. M. Shariff, *J. Membr. Sci.*, 2017, **525**, 175-186.

6. M. R. Khdhayyer, E. Esposito, A. Fuoco, M. Monteleone, L. Giorno, J. C. Jansen, M. P. Attfield, P. M. Budd, *Sep. Purif. Technol.,* 2017, **173**, 304-313.

7. A. F. Bushell, M. P. Attfield, C. R. Mason, P. M. Budd, Y. Yampolskii, L. Starannikova, A. Rebrov, F. Bazzarelli, P. Bernardo, J. C. Jansen, M. Lanč, K. Friess, V. Shantarovich, V. Gustov, V. J. Isaeva, *Membr. Sci.,* 2013, **427**, 48-62.

8. M. Shan, B. Seoane, E. Rozhko, A. Dikhtiarenko, G. Clet, F. Kapteijn, J. Gascon, *Chem. Eur. J.*, 2016, **22**, 14467-14470.

9. E. V. Perez, K. J. Balkus Jr., J. P. Ferraris, I. H. Musselman, *J. Membr. Sci.,* 2009, **328**, 165-173.